

RSC Advances



This is an *Accepted Manuscript*, which has been through the Royal Society of Chemistry peer review process and has been accepted for publication.

Accepted Manuscripts are published online shortly after acceptance, before technical editing, formatting and proof reading. Using this free service, authors can make their results available to the community, in citable form, before we publish the edited article. This *Accepted Manuscript* will be replaced by the edited, formatted and paginated article as soon as this is available.

You can find more information about *Accepted Manuscripts* in the [Information for Authors](#).

Please note that technical editing may introduce minor changes to the text and/or graphics, which may alter content. The journal's standard [Terms & Conditions](#) and the [Ethical guidelines](#) still apply. In no event shall the Royal Society of Chemistry be held responsible for any errors or omissions in this *Accepted Manuscript* or any consequences arising from the use of any information it contains.

1 **Low thermal conductivity nitrogen-doped graphene aerogels for thermal insula-**
2 **tion**

3 Chenwu YUE, Jian FENG*, Junzong FENG, Yonggang JIANG

4 *Science and Technology on Advanced Ceramic Fibers and Composites Laboratory,*
5 *National University of Defense Technology, Changsha 410073, China*

6 **Abstract:** Aerogels, like SiO₂ aerogels, Al₂O₃ aerogels and carbon aerogels, have
7 been widely used in thermal insulation. However, graphene aerogels (or reduced gra-
8 phene oxide aerogels), with similar structure, have never been used in this field. In
9 this paper, the concept of suppressing graphene aerogels' thermal conductivity by in-
10 troducing defects or doping atoms in graphene was introduced. Nitrogen-doped
11 (N-doped) graphene aerogels with low thermal conductivity were prepared with par-
12 aphenylene diamine as bridging and doping agent by CO₂ supercritical drying. With
13 the introduction of doping atoms and bridging agent, the solid thermal conductivity is
14 depressed. Also, with CO₂ supercritical drying, the pore size is reduced and the gase-
15 ous thermal conductivity is suppressed. The lowest thermal conductivity of N-doped
16 graphene aerogels is 0.023 W/(m K), which is nearly 1/2 of that ever reported and
17 which is even lower than that of static air. Meanwhile, the thermal insulation mecha-
18 nisms were also studied. The low thermal conductivity and low bulk density make
19 N-doped graphene aerogels a potentially useful thermal insulation material that may
20 significantly lighten thermal insulation system.

21 **Key words:** graphene, doping, aerogels, thermal conductivity, thermal insulation

* Corresponding author. Tel: +86 0731 84576291. Fax: +86 0731 84576578. E-mail: fengj@nudt.edu.cn.

22 1. Introduction

23 With nanoporous structure, high porosity and low density^[1], aerogels have been
24 widely used in thermal insulation^[2]. Their nanoporous structure suppresses gaseous
25 thermal conductivity^[3], low density depresses solid thermal conductivity^[4]. For ex-
26 ample, SiO₂ aerogels^[2], Al₂O₃ aerogels^[5] and carbon aerogels^[6] et al. Compared with
27 these aerogels, graphene aerogels have similar structure, lower density, higher
28 strength and perfect opacity. The opacity can lower radiant thermal conductivity,
29 hence may further reduced their thermal conductivity. Although with these characters,
30 graphene aerogels have never been used in thermal insulation. The most crucial rea-
31 son for this should be the superhigh thermal conductivity of graphene.

32 Graphene is a single atomic layer of sp² carbon atoms^[7,8]. It has received much atten-
33 tion since first obtained by mechanical exfoliation^[6] for its excellent electrical^[9],
34 thermal^[10], optical^[11] and mechanical^[12] properties. Its measured values of thermal
35 conductivity at room temperature for suspended samples are as high as 2500-5300
36 W/(m K)^[13,14].

37 However, defects and doping atoms in graphene may significantly impact its thermal
38 conductivity^[15,16]. Several groups have studied the effects of different kinds of defects
39 (variety of vacancy^[17-19] and doping^[20,21]) on its thermal conductivity by computer
40 simulation using force constant method^[22], molecular dynamics method^[23] and
41 Green's function method^[17] et al. They found the thermal conductivity of graphene
42 sharply decreases with the amount of defects or doping atoms increasing. Taking the
43 fact that the thermal conductivity of graphene oxide is only 3.19W/(m K) compared

44 with graphene (5300 W/(m K)), the thermal conductivity of graphene can be de-
45 scended by introducing a great amount of defects or doping atoms.

46 Zhong^[24] reported the thermal conductivity of graphene aerogels (reduced graphene
47 oxide (rGO) aerogels) prepared by hydrothermal reduction and freeze-drying for the
48 first time. The thermal conductivity measured with laser flash technique is as high as
49 2.183 W/(m K). Their bulk density and surface area are 227mg/cm³ and 43m²/g, re-
50 spectively. Fan^[25,26] studied the effects of thermal treatment on the thermal conductiv-
51 ity of graphene aerogels (rGO aerogels) by infrared microscopy technique. The aero-
52 gels were prepared by CO₂ supercritical drying. This reduces their pore size and hence
53 decreases the gaseous thermal conductivity. But the thermal conductivity of graphene
54 aerogels before and after thermal treatment at 450°C for 5h are still 0.12~0.36
55 W/(m K) and 0.18~0.31 W/(m K), respectively. And their bulk density is
56 14.1~52.4mg/cm³ and 16.4~49.0mg/cm³, respectively. Tang^[27] synthesized graphene
57 aerogels (rGO aerogels) with paraphenylene diamine (PPD) as reducing and function-
58 alizing agent in the presence of ammonia (NH₃·H₂O) by freeze-drying, and charac-
59 terized the thermal conductivity of the aerogels using Hot Disk Techmax TPS1500
60 thermal meter. The thermal conductivity with bulk density from 1.8mg/cm³ to
61 27.2mg/cm³ is 0.040~0.053 W/(m K). Since the use of freeze-drying, the pore size of
62 the aerogels is relatively bigger. So the thermal conductivity can be further depressed
63 by reducing the pore size.

64 In this paper, the concept of decreasing graphene aerogels' thermal conductivity by
65 introducing defects and (or) doping atoms to graphene was introduced. By introducing

66 doping atoms, together with reducing pore size by CO₂ supercritical drying, N-doped
67 graphene aerogels with low thermal conductivity was obtained. These aerogels are
68 potentially useful in thermal insulation for their low thermal conductivity and low
69 bulk density.

70 **2. Experimental section**

71 2.1 materials

72 Graphene oxide (GO) aqueous suspension (15 mg/ml) was bought from Nanjing
73 Jicang nanotechnology Co. Ltd. GO suspension with other concentration was obtained
74 by diluting the aqueous suspension with deionized water. PPD were purchased from
75 Sinopharm Chemical Reagent Co. Ltd. Ethanol and concentrated NH₃·H₂O were ob-
76 tained from Hunan Hengyang Kaixin Chemical Co. Ltd. All the chemicals were used
77 as received without further purification.

78 2.2 Synthesis of graphene aerogels

79 100 ml GO suspension (3, 6, 9, 12, 15 mg/ml, for a typical procedure it is 12 mg/ml)
80 was commixed with X g PPD and 2.7 ml concentrated NH₃·H₂O (The X were 1.2, 2.4,
81 3.6, 4.8, 6.0, respectively, for a typical procedure it is 4.8). Subsequently, The mixture
82 was heated at 90 °C for 8 h to gain N-doped graphene hydrogels. Then the solvent in
83 the hydrogel was exchanged with water and ethanol for 5 times, respectively. Finally,
84 the gel was dried with supercritical CO₂ to form N-doped graphene aerogels.

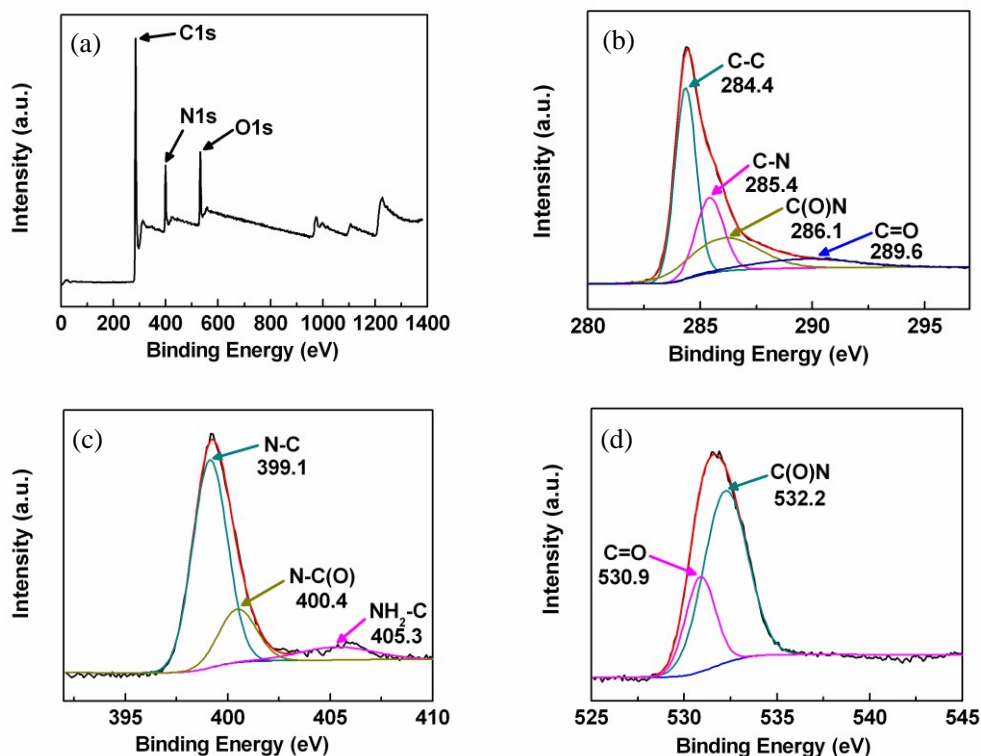
85 2.3 Characterization

86 The bulk density was calculated from the mass and corresponding volume. The mi-
87 crostructure was observed with Hitachi S4800 field emission scanning electron mi-

88 croscope (SEM). The surface composition was characterized in TESCALAB 250Xi
89 X-ray photoelectron spectroscope (XPS). The nitrogen adsorption-desorption tests
90 were carried out at 77 K in autosorb-1 physical adsorption instrument after 16 hours
91 of sample outgassing in vacuum, and the specific surface area and pore size distribu-
92 tion were calculated by the BET (Brunauer–Emmett–Teller) method and BJH (Bar-
93 rett–Joyner–Halenda) method, respectively. The thermal conductivity was measured
94 with samples $\Phi 39\sim 42 \times 15$ mm using Hot Disk TPS2500 apparatus by the 5465
95 sensor.

96 **3. Results and discussion**

97 During the heat preservation, N-doped graphene hydrogels are obtained by PPD
98 grafting with GO sheets and π - π stacking between reduced graphene oxide sheets^[27].
99 The GO sheets are simultaneously reduced and functionalized by PPD. From the XPS
100 spectra (Fig. 1), N atoms and O atoms respectively account for 13.34 %at and
101 9.98 %at in the sample (table 1), illustrating the introducing of PPD into as-prepared
102 N-doped graphene aerogels. According to the C 1s XPS spectra (Fig. 1(b)) of
103 as-prepared N-doped graphene aerogels, the peaks at 285.4 eV corresponding to C-N
104 and 286.1 eV corresponding to C(O)N indicate the covalent bonding of PPD to gra-
105 phene sheets. This can be further proved by the peaks at 399.1 eV and 400.4 eV from
106 N 1s XPS spectra (Fig. 1(c)) and peak at 532.2 eV from O 1s XPS spectra (Fig. 1(d)).



107

108 Fig. 1 (a) Broad XPS spectra, (b) C 1s spectra, (c) N 1s spectra and (d) O 1s spectra of

109

as-prepared N-doped graphene aerogels

110

111

Table 1 Element percentage of as-prepared N-doped graphene aerogels

Element	C	O	N
Content (%at)	76.68	9.98	13.34

112

113 However, different with freeze drying, the porous network is fully preserved after CO₂

114 supercritical drying. Fig. 2 is the SEM micrograph of as-prepared N-doped graphene

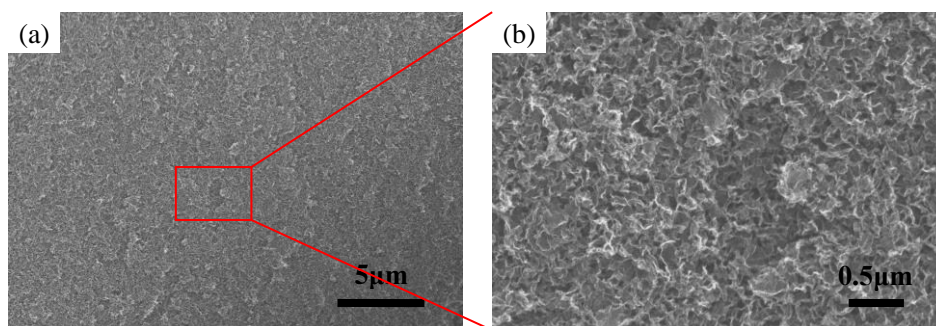
115 aerogels. As shown in the image, the N-doped graphene sheets randomly intercon-

116 nected with each other, forming pores in several dozens or hundreds nanometers. The

117 size of the pores is much smaller than that of N-doped graphene aerogels prepared by

118 freeze drying (Fig. 3). The microstructure of as-prepared N-doped graphene aerogels

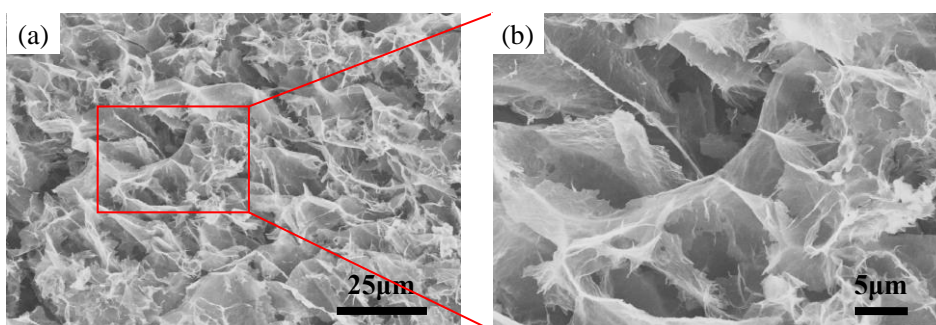
119 is homogeneous to some extent.



120

121

Fig. 2 SEM micrograph of as-prepared N-doped graphene aerogels



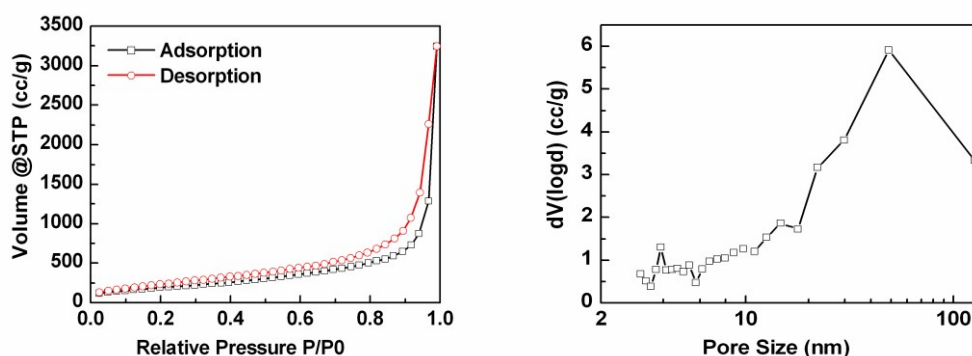
122

123 Fig. 3 SEM micrograph of as-prepared N-doped graphene aerogels by freeze drying

124

125 The N_2 adsorption-desorption isotherm curve and BJH pore size distribution of
126 as-prepared N-doped graphene aerogels with bulk density 34.5 mg/cm^3 are shown in
127 Fig. 4. The isotherm curve belongs to typical type III adsorption-desorption iso-
128 therm^[28], revealing plenty of pores with size more than 5 nm and wide range of pore
129 sizes. The result is consistent to the result of SEM micrograph. Also, the adsorption
130 capacity is really large, showing the great pore volume. According to the BJH pore
131 size distribution, most of the pore diameter is larger than 10 nm, which reaches their
132 maximum at 49 nm. This can further prove the result from SEM micrograph. The pore
133 volume see downward tendency with the pore diameter increasing to 140 nm, but the
134 volume of pore with sizes bigger than 140 nm is still great. Those pores cannot be ex-

135 plored by N₂ adsorption-desorption test but can be observed from the SEM micro-
 136 graph. According to the bulk density of as-prepared N-doped graphene aerogels
 137 (11.1~35.0 mg/cm³, Table 2), the pore volume may be 28~89 cm³/g compared with
 138 3.26~5.88 cm³/g by BJH method based on N₂ adsorption-desorption isotherm curves.



139
 140 Fig. 4 N₂ adsorption-desorption isotherm curve and BJH pore size distribution of
 141 as-prepared N-doped graphene aerogels

142
 143 Table 2 The textural properties of as-prepared N-doped graphene aerogels with varied
 144 bulk density

GO concentration (mg/ml)	Bulk density (mg/cm ³)	BET surface area (m ² /g)	Pore volume (cm ³ /g)
3	11.1±0.7	568.7	3.26
6	19.9±0.6	705.5	4.93
9	24.7±1.1	802.4	4.90
12	34.5±1.0	891.7	5.88
15	35.0±1.1	751.7	4.15

145 At the same time, shrinkage of 1 %~8 % in sample diameter with the variation of GO

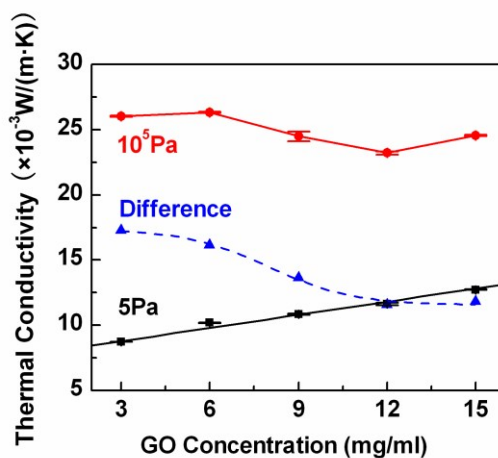
146 concentration was observed during CO₂ supercritical drying. That may attribute to the
147 surface tension during drying, although which is relatively weak due to the super-
148 critical state of resolve. But the shrinkage does not impact the structure and appear-
149 ance of as-prepared N-doped graphene aerogels, without crack being noted from the
150 photograph (Fig. 5) and the micrograph (Fig. 2).



151

152

Fig. 5 Photograph of as-prepared N-doped graphene aerogels



153

154

Fig. 6 Thermal conductivity of as-prepared N-doped graphene aerogels

155

156 Fig. 6 shows the thermal conductivity of as-prepared N-doped graphene aerogels with
157 varied GO concentration. With the GO concentration increasing from 3 mg/ml to 12
158 mg/ml, the thermal conductivity of as-prepared N-doped graphene aerogels at room
159 temperature (25 °C) and atmospheric pressure (10⁵ Pa) shows decrease tendency. But

160 with the GO concentration continues to increase to 15 mg/ml, the thermal conductivity
161 increases a little. When the GO concentration is 12 mg/ml, the thermal conductivity is
162 only 0.023 W/(m K). The thermal conductivity at room temperature and 5 Pa see a
163 different trend. The thermal conductivity almost linearly increases with the GO con-
164 centration increasing. The higher GO concentration increases the bulk density of
165 as-prepared N-doped graphene aerogels. This reinforces the juncture of graphene
166 sheets and magnifies the solid content in unit volume. Since graphene sheets are the
167 carrier of heat transmission, the solid thermal conductivity increases. With the radiant
168 thermal conductivity at this temperature and the gaseous thermal conductivity at 5 Pa
169 both negligible, the thermal conductivity at room temperature and 5 Pa is mostly con-
170 sist of solid thermal conductivity. So, the thermal conductivity of as-prepared
171 N-doped graphene aerogels at 5 Pa increases with the increasing of GO concentration.
172 Differently, the difference between thermal conductivity at atmospheric pressure and
173 that at 5 Pa narrows down. The difference matches very well with the inverse S-curve.
174 The reason for that is the difference mainly makes up of gaseous thermal conductivity.
175 The enhancement of bulk density caused by the increase of the GO concentration de-
176 creases the pore size of as-prepared N-doped graphene aerogels (Fig. S11, Fig. 2).
177 Hence the gaseous thermal conductivity was restrained more thoroughly. When the
178 GO concentration is relatively low (< 6 mg/ml), the pore size is relatively great. Its
179 restrain to gaseous thermal conductivity is not so significant. Meanwhile, when the
180 GO concentration is relatively high (> 12 mg/ml), the effect of GO concentration on
181 bulk density diminishes. Hence, the relationship between GO concentration and gas-

182 eous thermal conductivity lighten. So, with the increase of the GO concentration, the
 183 difference (namely, gaseous thermal conductivity) shows an inverse S-curve. Logi-
 184 cally, the linear increase of the thermal conductivity at 5Pa and the nonlinear decrease
 185 of the difference (the gaseous thermal conductivity) inducing the variation of the
 186 thermal conductivity of as-prepared N-doped graphene aerogels at atmospheric pres-
 187 sure.

188 Table 3 Thermal conductivity of rGO aerogels

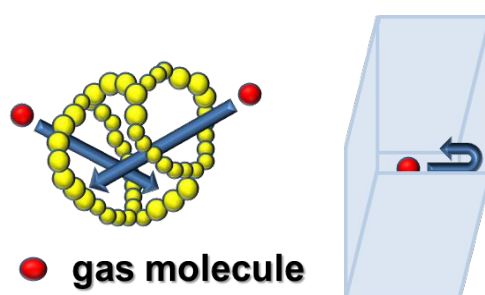
author	Bulk density (mg/cm ³)	BET surface area (m ² /g)	Thermal conductivity (W/(m K))	Reference
Yajuan Zhong	227	43	2.183	[24]
Zeng Fan	14.1~52.4	-	0.12~0.36	[25], [26]
Gongqing Tang	1.8~27.2	-	0.040~0.053	[27]
Chenwu Yue	11.1~35.0	568~892	0.023~0.026	This work

189
 190 Compared with that from public articles (Table 3), the thermal conductivity of
 191 as-prepared N-doped graphene aerogels is significantly lower, which is nearly half of
 192 the minimum value ever reported. Four reasons may contribute to this result.

193 First, just as reported by Fan^[26] et al, the defects in graphene and the relatively small
 194 size of graphene sheets limit the transmission of heat, and hence reduces the thermal
 195 conductivity of as-prepared N-doped graphene aerogels to some extent.

196 Second, the CO₂ supercritical drying sharply diminishes the pore size in as-prepared
 197 N-doped graphene aerogels. According to the computation by BJH method based on
 198 N₂ adsorption-desorption curve, most of the pores centralize on 49 nm. It is shorter

199 than the mean molecule freedom path ($\sim 70 \text{ nm}^{[3]}$) at room temperature and atmos-
200 pheric pressure, and hence can obviously depress the gaseous thermal conductivity.
201 The research of Feng^[29] et al shows that the gaseous thermal conductivity will be cru-
202 cially suppressed, if only the pore diameter smaller than 2 times of the mean molecule
203 freedom path (namely 140nm at room temperature and atmospheric pressure). So the
204 gaseous thermal conductivity is reduced. Besides, the 2-dimension structure of gra-
205 phene sheets may effectively block off the transfer of gas molecules like the wall
206 compared with other aerogels (such as SiO_2 aerogels, Al_2O_3 aerogels, carbon aerogels
207 et al) with 3-dimension open-cell network structure (Fig. 7). Hence graphene aerogels
208 can greatly suppress the gaseous heat transmission through gas molecular collision.
209 With these 2 mechanisms the gaseous thermal conductivity of as-prepared N-doped
210 graphene aerogels is significantly depressed.



211

212 Fig. 7 Schematic diagram of aerogels with open-cell network structure (left) and

213

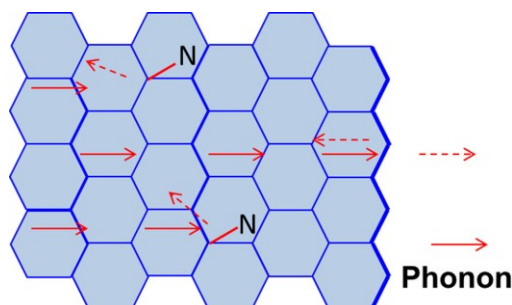
as-prepared N-doped graphene aerogels (right)

214

215 Third, the introduction of doping atoms turns sp^2 carbon to sp^3 carbon, destroying the216 perfect π -electron conjugated structure and crystal structure, which are the main path

217 heat transmitting through graphene. Phonons are the main carrier of heat delivering in

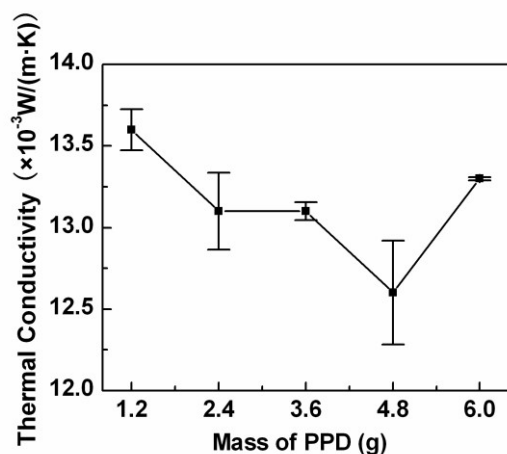
218 graphene, which transfer heat by lattice vibration. With the introduction of doping
219 atoms, the crystal structure of doping graphene is divided into smaller pieces by sp³
220 carbon atoms (namely carbon chemically linked with doping atoms (Fig. 1(b), the
221 peaks at 285.4 eV and 286.1 eV)). The scattering of phonons on these obstacles to-
222 gether with the defects and edge can significantly diminish the amount of heat passing
223 through the doping graphene (Fig. 8). Meanwhile, electrons are the other carrier of
224 heat delivering in graphene, which transfer heat by electron travelling. With the dop-
225 ing atoms introduced, the intactness of π -electron conjugated structure is broken, the
226 resistance of electron motion boosting. As a result, the heat transferred through elec-
227 tron travelling is reduced. By this way, the solid thermal conductivity of as-prepared
228 N-doped graphene aerogels is further debased. Fig. 9 is the thermal conductivity (5 Pa)
229 of as-prepared N-doped graphene aerogels (GO is 12 mg/ml) with varied PPD mass.
230 When PPD mass is no more than 4.8 g, the thermal conductivity at 5 Pa decreases
231 with the increasing of PPD mass. Since the increasing of PPD mass increases the
232 amount of N doped to the sample, the as-prepared N-doped graphene aerogels with
233 more PPD show better thermal insulation performances at 5 Pa.



234

235

Fig. 8 Schematic diagram of as-prepared N-doped graphene aerogels



236

237 Fig. 9 Thermal conductivity (5Pa) of as-prepared N-doped graphene aerogels with
238 varied PPD mass

239 Fourth, PPD also plays a role like bridging agent. It linked doping graphene with each
240 other. With the introduction of bridging agent, the heat transferring between the gra-
241 phene is significantly limited even if that through graphene could have been greater.
242 The bridging agent crucially restricts the heat flux like bottleneck. Therefore, the heat
243 pass through the as-prepared N-doped graphene aerogels is reduced and the solid
244 thermal conductivity ulteriorly gets fallen. According to Fig. 9, the increasing of
245 thermal conductivity (5 Pa) when PPD mass is 6.0 g illustrates the increase of the
246 amount of 'bridges' accelerating the heat transfer to some extent.

247 With the above four reasons, the thermal conductivity of as-prepared N-doped gra-
248 phene aerogels is really low, which is even lower than that of static air (0.026
249 W/(m K))^[30]. The low thermal conductivity ($0.023\sim 0.026 \text{ W/(m K)}$) and low bulk
250 density ($11.1\sim 35.0 \text{ mg/cm}^3$) are crucially important for the use of N-doped graphene
251 aerogels in thermal insulation. And the use of this material may significantly lighten
252 the weight of thermal insulation system. Meanwhile, the gaseous thermal conductivity

253 of N-doped graphene aerogels still takes up a great proportion among the thermal
254 conductivity. That may be because the percentage of pore with relatively bigger size
255 (>140 nm) is still considerable. So the thermal conductivity of N-doped graphene
256 aerogels may be further depressed by ulteriorly narrowing the pore size.

257

258 **4. Conclusion**

259 We introduced the concept of lowering the thermal conductivity of graphene aerogels
260 by introducing defects or doping atoms in graphene, and prepared
261 low-thermal-conductivity N-doped graphene aerogels using PPD as bridging and
262 doping agent by CO₂ supercritical drying. The PPD is anchored in graphene sheets
263 during reaction. By CO₂ supercritical drying, the pore sizes of as-prepared N-doped
264 graphene aerogels are much smaller than that by freeze drying. Remarkably, the low-
265 est thermal conductivity of as-prepared N-doped graphene aerogels is only 0.023
266 W/(m K), even lower than that of static air, showing good thermal insulation perfor-
267 mances. The reasons are: (1) The transmission of heat is limited by the defects in
268 graphene and the relatively small size of graphene sheets; (2) The relatively smaller
269 pore size and 2-dimension structure of graphene sheets suppress the gaseous thermal
270 conductivity; (3) The introduction of doping atoms boosting the scattering of phonon,
271 greatly depresses the solid thermal conductivity; (4) The bridging agent restricts the
272 heat flux like bottleneck, further lowering the thermal conductivity. With low bulk
273 density (11.1~35.0 mg/cm³) and low thermal conductivity (0.023~0.026 W/(m K)),
274 the as-prepared N-doped graphene aerogels are potentially useful in thermal insulation,

275 and may significantly lighten the weight of thermal insulation system.

276 **Acknowledgements**

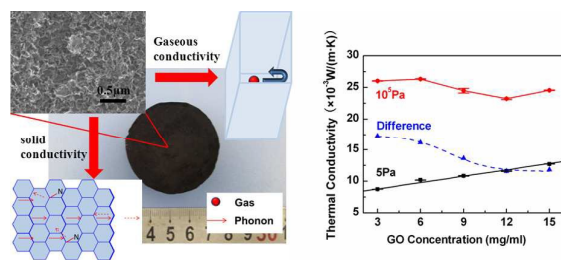
277 Thanks for the support from National Natural Science Foundation (51172279,
278 51302317) of China, Aid Program for Science and Technology Innovative Research
279 Team in Higher Educational Institutions of Hunan Province and Aid Program for In-
280 novative Group of National University of Defense Technology.

281 **References**

- 282 [1] N. Hüsing and U. Schubert, *Angew Chem Int Ed*, 1998, **37**, 22-45;
- 283 [2] J. Feng, Q. Gao, J. Feng and Y. Jiang, *Journal of National University of Defense*
284 *Technology*, 2010, **32**, 40-44;
- 285 [3] X. Lu, M. C. Arduini-Schuster and J. Kuhn, *Science*, 1992, **255**, 971-972;
- 286 [4] S. N. Schiffres, K. H. Kim, L. Hu, A. J. H. McGaughey, M. F. Islam and J. A.
287 Malen, *Adv Funct Mater*, 2012, **22**, 5251-5258;
- 288 [5] Q. Gao, C. Zhang, J. Feng, W. Wu, J. Feng and Y. Jiang, *Chinese Journal of Inor-*
289 *ganic Chemistry*, 2008, **24**, 1456-1460;
- 290 [6] J. Feng, J. Feng and C. Zhang, *J Porous Mater*, 2012, **19**, 551-556;
- 291 [7] K. S. Novoselov, A. K. Geim, S. V. Morozov, D. Jiang, Y. Zhang, S. V. Dubonos, I.
292 V. Grigorieva and A. A. Firsov, *Science*, 2004, **306**, 666-669;
- 293 [8] D. C. Marcano, D. V. Kosynkin, J. M. Berlin, A. Sinitskii, Z. Sun, A. Slesarev, B.
294 A. Lawrence, L. Wei and M. T. James, *ACS NANO*, 2010, **8**, 4806-4814;
- 295 [9] D. Basu, M. Gilbert, L. Register, S. Banerjee and A. MacDonald, *Appl Phys Lett*,
296 2008, **92**, 042114;

- 297 [10] A. A. Balandin, S. Ghosh, W. Bao, I. Calizo, D. Teweldebrhan, F. Miao and C. N.
298 Lau, NANO Letters, 2008, **8**, 902-907;
- 299 [11] M. Liu, X. Yin, E. Ulin-Avila, B. Geng, T. Zentgraf, L. Ju, F. Wang and X.
300 Zhang, Nature, 2011, **474**, 64-67;
- 301 [12] A. K. Geim, Science, 2009, **324**, 1530-1534;
- 302 [13] S. Ghosh, W. Bao, D. L. Nika, S. Subrina, E. P. Pokatilov, C. N. Lau and A. A.
303 Balandin, Nat Mater, 2010, **9**, 555-558;
- 304 [14] W. Cai, A. L. Moore, Y. Zhu, X. Li, S. Chen, L. Shi and R. S. Ruoff, Nano Lett,
305 2010, **10**, 1645-1651;
- 306 [15] P. Yang, X. Wang, P. Li, H. Wang, L. Zhang and F. Xie, Acta Phys Sin, 2012, **61**,
307 076501;
- 308 [16] W. Yu, H. Xie and X. Wang, Journal of Engineering Thermophysics, 2012, **33**,
309 1609-1611;
- 310 [17] H. Zhang, L. Geunsik and C. Kyeongjae, Physical Review B, 2011, **84**, 115460;
- 311 [18] H. Justin, K. Alper, S. Cem, S. Haldun, C. Gianarelio and C. Tahir, ACS
312 NANO, 2011, **5**, 3779-3787;
- 313 [19] Y. Y. Zhang, Y. Cheng, Q. X. Pei, C. M. Wang and Y. Xiang, Physics Letters A,
314 2012, **376**, 3668-3672;
- 315 [20] L. Wang and H. Sun. J Mol Model, 2012, **18**, 4811-4818;
- 316 [21] Z. Hui, P. He, Y. Dai and A. Wu, Acta Phys Sin, 2014, **63**, 074401;
- 317 [22] K. Hossein, N. Neophytos, P. Mahdi and K. Hans, J Comput Electron, 2012, **11**,
318 14-21;

- 319 [23] N. Khosravian, M. K. Samani, G. C. Loh, G. C. K. Chen, D. Baillargeat and B. K.
320 Tay, Computational Materials Science, 2013, **79**, 132-135;
- 321 [24] Y. Zhong, M. Zhou, F. Huang, T. Lin and D. Wan, Solar Energy Materials &
322 Solar Cells, 2013, **113**, 195-200;
- 323 [25] Z. Fan, D. Z. Y. Tng, C. X. T. Lim, P. Liu, S. T. Nguyen, P. Xiao, A. Marconnet,
324 C. Y. H. Lim and H. M. Duong, Colloids and Surfaces A: Physicochem Eng Aspects,
325 2014, **445**, 48-53;
- 326 [26] Z. Fan, A. Marconnet, S. T. Nguyen, C. Y. H. Lim and H. M. Duong, Interna-
327 tional Journal of Heat and Mass Transfer, 2014, **76**, 122-127;
- 328 [27] G. Tang, Z. Jiang, X. Li, H. Zhang, A. Dasari and Z. Yu, CARBON, 2014, **77**,
329 592-599;
- 330 [28] F. Rouquerol, J. Rouquerol and K. Sing, Adsorption by powders and porous solid,
331 principles, methodology and applications, Academic Press, 1999;
- 332 [29] J. Feng, J. Feng, Y. Jiang and C. Zhang, Aerospace Materials & Technology,
333 2012, **42**,1-6;
- 334 [30] R. Singh and H. S. Kasana, Appl Therm Eng, 2004, **24**, 1841-1849.



N-doped graphene aerogels with low thermal conductivity were prepared for the first time